MOLECULAR PHYSICS, 1995, VOL. 85, NO. 5, 1017–1032

Adsorption–desorption kinetics in nanoscopically confined oligomer films under shear

By E. MANIAS, A. SUBBOTIN†, G. HADZIIOANNOU and G. TEN BRINKE

Polymer Science Lab. and Materials Science Centre, University of Groningen, Nijenborgh 4, 9747 AG Groningen, The Netherlands

(*Received 7 March 1995; revised version accepted 5 May 1995*)

The method of molecular dynamics computer simulations is employed to study oligomer melts confined in ultra-thin films and subjected to shear. The focus is on the self-diffusion of oligomers near attractive surfaces and on their desorption, together with the effects of increasing energy of adsorption and shear. It is found that the mobility of the oligomers near an attractive surface is strongly decreased. Moreover, although shearing the system forces the chains to stretch parallel to the surfaces and thus increase the energy of adsorption per chain, flow also promotes desorption. The study of chain desorption kinetics reveals the molecular processes responsible for the enhancement of desorption under shear. They involve sequences of conformations starting with a desorbed tail and proceeding in a very fast, correlated, segment-by-segment manner to the desorption of the oligomers from the surfaces.

1. Introduction

An understanding of wear, friction, lucrication and adhesion is essential for the development of new materials and devices. Given the ever increasing miniaturization in technology, scientific interest has shifted towards the study of the behaviour of nanoscale systems. In this respect, the rheology of strongly confined lubricants is of immense importance in particular, because it differs in many ways from the corresponding bulk systems. Recent rapid progress in experimental methods, such as the atomic force microscope (AFM) and the surface forces apparatus (SFA) [1–5], provide researchers with the ability to study experimentally such systems and reveal very rich and often striking behaviour at the molecular scale.

These kinds of experiment are very naturally complemented by computer simulations ranging from simple lattice studies [6] and equilibrium molecular dynamics (MD) [7] to nonequilibrium MD for studying shear [8] and MD of confined realistic short alkanes [9]. Molecular simulations, though addressing smaller systems than the SFA, not only manage to capture many of the experimental findings but also help to further our insight into the molecular processes responsible for the macroscopic experimental observations. Thus, the experimental findings, involving the dramatic changes that take place when systems are confined in nanometric distances between strongly physisorbing surfaces (usually mica), can be correlated with microscopic/molecular processes. The anomalous behaviour of a quantized stepwise squeezing of a film [10, 11] is connected with the fact that the confined

† Permanent address: Institute of Petrochemical Synthesis, Russian Academy of Sciences, Moscow 117912, Russia.

systems exhibit layering next to a surface [12, 7], and that this layering is of the same nature as in the radial distribution function of liquids [13]. Moreover, these nanoscopically confined films are characterized by much higher (up to three orders of magnitude) effective viscosities than the bulk systems [14], and when subjected to flow shear thinning starts at much smaller shear rates than in macroscopic films following a simple power law [3]. MD simulations are in very good agreement with these findings [8]. Furthermore, when shear is imposed on films confined between very attractive surfaces (e.g., mica) their dynamics vary from liquid-like for wide films [5, 14, 3] to solid-like for film thicknesses smaller than 4 or 5 molecular diameters [2, 15], which can be explained by the dramatic slowdown of the segment dynamics inside the interface of a strongly adsorbing surface and a fluid [16]. Furthermore, studies of monomeric fluids in nanoscopic confinements under flow correlate the transitions between the liquid-like and solid-like response to shear with changes in the in-plane ordering near the wall [17]; when particle exchange is allowed, this behaviour is correlated with changes in the wall registry and the order within the film, and also with changes in the number of particles [18].

All of this indicates the importance of the structural and dynamical changes taking place inside the solid–fluid interface, which can determine the response of the entire film for sufficiently thin films. In this paper we focus on how shear affects the mobility and desorption of oligomers near attractive surfaces. Preliminary results [19] for confined systems of hexamers showed that the centre of mass diffusivity normal to the walls increases with shear rate, although the average energy of adsorption per chain increases. In this study we investigate this problem further and simulate systems with longer chains, namely decamers, and describe the molecular mechanism responsible for this *shear enhanced desorption.*

2. MD simulation method

The systems studied in this paper are films of oligomers with 6 (hexamers) or 10 (decamers) segments per chain. The chains are modelled by a well studied bead spring model [20] confined between two double-layered (111) fcc surfaces normal to **z**, and periodic boundary conditions are imposed in the two other directions. Shear is imposed by moving the walls with a constant velocity (v_w) in opposite directions ($\pm\mathbf{x}$). The segments of the chains interact with each other via a purely repulsive, shifted and truncated Lennard-Jones (LJ) potential:

$$U(r) = \begin{cases} 4\epsilon\left(\left(\frac{\sigma}{r}\right)^{12} - \left(\frac{\sigma}{r}\right)^{6} + \frac{1}{4}\right), & r \leqslant \sqrt[6]{(2)}\sigma \\ 0, & r > \sqrt[6]{(2)}\sigma, \end{cases} \tag{1}$$

where ϵ is the LJ energy parameter, and σ the LJ length parameter. Connectivity is ensured by adding a strongly attractive finite extensibility non-elastic (FENE) potential between successive beads in one chain:

$$U_{\text{bond}}(r) = -\frac{k}{2} R_0^2 \ln\left(1 - \left(\frac{r}{R_0}\right)^2\right), \quad r < R_0, \tag{2}$$

where $R_0 = 1{\cdot}5\sigma$, and $k = 30{\cdot}0\epsilon/\sigma^2$. These potentials were used before in extensive studies of bulk systems [21], under confinement between walls [7, 16], as well as under shear [8, 22], and reproduce many static and dynamic properties of polymer

systems. Furthermore, the choice of parameters for the FENE potential has been shown to prevent bond crossing at the temperature used in our simulation [21]. The interactions between the wall particles and the segments are modelled by the *full* LJ potential, which includes an attractive tail:

$$U_w(r) = 4\epsilon_w\left(\left(\frac{\sigma_w}{r}\right)^{12} - \left(\frac{\sigma_w}{r}\right)^{6}\right). \tag{3}$$

In order to reduce the computational effort this potential is truncated at $r_{wc} = 2{\cdot}5\sigma$. By changing the value of ϵ_w the strength of the wall attraction can be varied systematically. For wall attractions $\epsilon_w \leqslant 1{\cdot}0\epsilon$ there is only a slight slowing down of the molecular motions characterizing a 'weakly physisorbing' surface, whereas for $\epsilon_w = 2{\cdot}0\epsilon$ and $3{\cdot}0\epsilon$ the surfaces are 'strongly physisorbing' by inducing an increase in the longest relaxation time of the adsorbed oligomers (pentamers) by a factor of between 70 (for $\epsilon_w = 2{\cdot}0$) and 1500 (for $\epsilon_w = 3{\cdot}0$) [16].

The temperature is kept constant at $k_BT = 1{\cdot}0\epsilon$ by rescaling the velocities [23] in two different ways: (i) scaling only the components of the velocities normal to the direction of the flow, and (ii) scaling also the thermal part of the velocity component parallel to flow. In the second method the film is divided into slices and the flow velocity is defined in each slice by averaging and scaling self-consistently. For these chain molecules and for slices containing on average 15 particles the two methods give the same results for the velocity profiles and local temperatures within the accuracy of the simulation. During our simulations we do not allow the solid atoms to undergo any thermal motion around their equilibrium positions. A more 'realistic' thermostat would involve momentum exchange between a thermally stabilized wall and the confined system. This method is far more computationally demanding than the ones used here, and at the same time previous studies show that fixing the substrate atoms does not change the results obtained significantly [28].

The SFA setup developed in our laboratory [24] is equipped with a feedback system enabling the separation of the two mica plates to be kept constant. In order to mimic this geometry the distance between the two walls is constant in our MD simulations ($h = 6\sigma$). Although it is difficult to determine the thermodynamic conditions of a bulk system at equilibrium with this pore fluid, such a bulk system has the same temperature as the simulated film and a density very close to the density in the middle of the pore. Fixing the film thickness results in keeping the volume constant, and since the number of particles and the temperature are also constant we study a canonical ensemble (NVT). Although in principle the dynamical properties and the nonlinear transport coefficients can, and do, change when simulations are carried out under constant pressure (NPT simulations) [25], we expect that the desorption kinetics will not differ essentially when an NVT or NPT ensemble is used.

A variant of Verlet's algorithm [23, 27] is used to integrate the differential equations of motion with a time step of 0·00462 MD time units, and lists of neighbours [27] are used to reduce the computational costs. Initial conformations are taken from a lattice Monte Carlo algorithm [6], and are further equilibrated using an MD run until steady state flow is achieved. Subsequently, intensive productive runs are performed. The duration of these runs is in the range $0{\cdot}4$–$0{\cdot}6 \times 10^6$ time steps for the systems with $\epsilon_w = 1{\cdot}0$ and high shear rates, and $0{\cdot}8$–$1{\cdot}0 \times 10^6$ time steps for the systems with $\epsilon_w = 2{\cdot}0$ or $3{\cdot}0$ and systems with lower shear rates. For the lower shear rates longer runs are necessary, since the flow velocities are

screened by the thermal motion. For this reason MD simulations can be used to study systems under high shear rates, in the range of $10^8\ s^{-1}$ and higher [8], which are much higher than the shear rates that can be applied in SFA experiments [4] (up to $10^5\ s^{-1}$), but are of the same order of magnitude as those found in magnetic storage devices.

3. Simulation results

The structure and dynamics of the adsorbed chains are of vital importance for the characterization of the nanoscopically confined systems, and determine to a great extent the dynamics of these systems [16]. When the attraction of the wall increases there is an enhancement of the inhomogeneity manifested by the increase of the first, and to a lesser extent of the second, layer density peak [19, 16]. Furthermore, for the hexamers the increase in the wall affinity (ϵ_w) favours conformations with many contacts with the walls at equilibrium (table 1). This should be attributed to the short size of the coils, as for the longer oligomers (decamers) at equilibrium, i.e., no flow, this effect is present to a much lesser extent (table 2).

Usually chains are grouped according to their centre of mass distance from the walls. However, recent studies [16, 19] show that a more physically justified grouping is based on the energy of adsorption per chain. Since the segment–segment potential is purely repulsive, ϵ_w can be considered as the excess solid atom–chain segment

Table 1. The probability of the adsorbed hexamers having one to six contacts (cont.) with the surfaces The wall velocity v_w is measured in MD units, and the wall to wall distance is $h = 6{\cdot}0\sigma$.

	v_w							
	0·00	0·10	0·20	0·30	0·50	0·90	1·5	2·0
				$\epsilon_w = 1{\cdot}0\epsilon$				
1 cont.	0·11	0·11	0·11	0·11	0·11	0·10	0·11	
2 cont.	0·17	0·16	0·15	0·15	0·13	0·11	0·11	
3 cont.	0·19	0·17	0·17	0·16	0·14	0·13	0·13	
4 cont.	0·18	0·17	0·19	0·18	0·17	0·17	0·16	
5 cont.	0·18	0·20	0·19	0·20	0·21	0·21	0·21	
6 cont.	0·16	0·19	0·20	0·21	0·24	0·28	0·29	
				$\epsilon_w = 2{\cdot}0\epsilon$				
1 cont.	0·07	0·08	0·05	0·08	0·05	0·05		0·05
2 cont.	0·11	0·09	0·08	0·10	0·07	0·06		0·05
3 cont.	0·14	0·13	0·14	0·14	0·10	0·05		0·06
4 cont.	0·17	0·19	0·17	0·15	0·12	0·08		0·07
5 cont.	0·22	0·20	0·24	0·19	0·17	0·18		0·12
6 cont.	0·30	0·31	0·32	0·34	0·48	0·58		0·63
				$\epsilon_w = 3{\cdot}0\epsilon$				
1 cont.	0·07	0·00	0·09	0·08	0·02	0·02		0·03
2 cont.	0·11	0·05	0·09	0·11	0·04	0·08		0·05
3 cont.	0·13	0·17	0·09	0·07	0·09	0·11		0·06
4 cont.	0·17	0·20	0·16	0·04	0·04	0·04		0·06
5 cont.	0·22	0·20	0·10	0·17	0·15	0·09		0·05
6 cont.	0·29	0·33	0·48	0·54	0·67	0·67		0·75

Table 2. The probability of the adsorbed decamers having one to ten contacts with the surfaces (v_w in MD units and $h = 6{\cdot}0\sigma$).

	Number of contacts									
v_w	1	2	3	4	5	6	7	8	9	10
					$\epsilon_w = 1{\cdot}0\epsilon$					
0·00	0·07	0·11	0·12	0·12	0·12	0·12	0·10	0·10	0·09	0·06
0·05	0·07	0·11	0·12	0·12	0·12	0·12	0·11	0·10	0·09	0·05
0·10	0·05	0·11	0·10	0·11	0·13	0·13	0·13	0·10	0·09	0·06
0·20	0·06	0·11	0·10	0·10	0·10	0·11	0·11	0·12	0·11	0·08
0·50	0·08	0·08	0·08	0·08	0·09	0·10	0·12	0·13	0·13	0·11
0·70	0·08	0·08	0·07	0·07	0·08	0·10	0·12	0·14	0·14	0·13
0·90	0·08	0·08	0·07	0·07	0·08	0·09	0·10	0·13	0·16	0·15
1·50	0·08	0·07	0·07	0·07	0·08	0·09	0·11	0·12	0·15	0·16
					$\epsilon_w = 2{\cdot}0\epsilon$					
0·00	0·05	0·06	0·11	0·14	0·14	0·11	0·11	0·09	0·08	0·09
0·10	0·03	0·08	0·08	0·09	0·08	0·10	0·13	0·13	0·13	0·14
0·20	0·05	0·06	0·06	0·04	0·03	0·06	0·09	0·15	0·21	0·24
0·40	0·04	0·04	0·05	0·04	0·04	0·08	0·11	0·14	0·20	0·26
0·50	0·04	0·05	0·05	0·05	0·07	0·07	0·10	0·15	0·19	0·24
0·60	0·04	0·05	0·07	0·08	0·04	0·03	0·05	0·10	0·17	0·38
0·70	0·04	0·04	0·03	0·04	0·04	0·06	0·07	0·13	0·19	0·36
0·90	0·04	0·04	0·04	0·06	0·04	0·04	0·06	0·09	0·16	0·43
1·50	0·05	0·05	0·04	0·03	0·03	0·04	0·04	0·06	0·13	0·52
					$\epsilon_w = 3{\cdot}0\epsilon$					
0·00	0·01	0·04	0·10	0·16	0·11	0·14	0·10	0·11	0·12	0·12

adhesive energy [16], and the number of contacts multiplied by the energy parameter of the wall potential (ϵ_w) is the energy of adsorption of a chain. An adsorbed segment, or contact, is defined as a segment located inside the first peak of the density profile [19, 22]. The probability of a certain energy of adsorption (i.e., a certain number of contacts) per chain is defined by the distribution of these quantities over all adsorbed chains, on both surfaces, and over time; these probabilities are given in tables 1 and 2.

The mobility of the chains is another very important quantity and can be measured through the centre of mass diffusion coefficients. Of course, due to confinement and flow the diffusion tensor is anisotropic and its two most interesting elements are the diffusion coefficient normal to the confining walls (D_{zz}), and the diffusion coefficient parallel to the surfaces but normal to flow (D_{yy}). These coefficients can be determined by the slope of the respective centre of mass mean-square displacements [19] since, by definition,

$$\langle (z(t) - z(0))^2 \rangle = 2D_{zz}t \tag{4}$$

and

$$\langle (y(t) - y(0))^2 \rangle = 2D_{yy}t.$$

At equilibrium (i.e., no flow) the mobility of chains with adsorbed segments is reduced in comparison with the free chains located in the middle of the pore (table 3). As expected, chains with more contacts are more strongly slowed down (table 3, [19, 16]), and the centre of mass mean-square displacements and diffusion coefficients have to be calculated separately for chains with different numbers of contacts.

Table 3. The centre of mass diffusion coefficients normal (D_{zz}) and parallel (D_{yy}) to the walls for systems of hexamers at equilibrium (no flow). The mobility of the free chains located in the middle of the film and of adsorbed chains with 2, 4, and 6 surface contacts (cont.) are presented. MD units are used throughout, and the width of the film is $h = 6{\cdot}0\,\sigma$.

ϵ_w	D_{zz}				D_{yy}			
	Free	2 cont.	4 cont.	6 cont.	Free	2 cont.	4 cont.	6 cont.
1·0	0·0052	0·0043	0·001 8	0·001 35	0·0190	0·0075	0·0067	0·0063
2·0	0·0047	0·0012	0·000 2	0·000 13	0·0191	0·0035	0·0012	0·0009
3·0	0·0052	0·0001	0·000 05	0·000 005	0·0192	0·0005	0·0004	0·0003

Depending on the wall affinity, the mobility of the adsorbed chains can be affected from a moderate slow down near a weakly physisorbing surface to decreases of many orders of magnitude near a strongly adsorbing wall. For example, for the full adsorbed hexamers (table 3), the diffusivities normal to the surfaces are reduced with respect to the chain mobility in the middle of the pore by a factor of less than 4 for $\epsilon_w = 1{\cdot}0$, by almost 40 times for $\epsilon_w = 2{\cdot}0$, and by to three orders of magnitude for $\epsilon_w = 3{\cdot}0$. These results are in very good agreement with the decrease in the segment mobility of pentamers in the vicinity of similar surfaces reported by Bitsanis and Pan [16]. As found before [26, 16], the mobility parallel to the surfaces is several times greater than that normal to the walls, and for the adsorbed chains is reduced to a lesser extent by the wall energetics; for the same chains, i.e. fully adsorbed hexamers, D_{yy} decreases by a factor of 3, 20, and 64 for $\epsilon_w = 1$, 2, and 3, respectively (table 3).

When shear is imposed there is a definite tendency for the adsorbed chains to stretch along the wall, thus adopting conformations with many contacts with the surfaces. This tendency gets stronger with increasing shear rate ($\dot{\gamma}$). For example the probability of a fully adsorbed chain (6 or 10 contacts with the surface) increases smoothly with $\dot{\gamma}$ (tables 1 and 2). This preference of the adsorbed chains to adopt conformations with many contacts under flow is observed both for the hexamers and the decamers, and is much stronger for the more attractive surfaces (tables 1 and 2). This means that the average energy of adsorption per chain is increasing with shear rate. On the other hand, the centre of mass diffusivity normal to the walls (D_{zz}) also increases with shear rate (table 4), i.e., desorption is enhanced by the flow even though the chains are bound to the surfaces with higher adsorption energies. The effect of shear on the self-diffusion of a bulk non-Newtonian fluid has been studied [29], and a dependence on shear rate was found to be of the type:

$$D_{aa} = D^0 + D^1_{aa}\dot{\gamma}^n, \tag{5}$$

with $n = 1/2$. We fitted the same type of power law to our diffusivities for the free chains located in the middle of the film, and we found that n is approximately 1/2. So, in figure 1 we plot the diffusivities normal and parallel to the walls versus the square root of the local shear rate ($\dot{\gamma}_{middle} = (\partial u_x/\partial z)_{middle}$).

In order to get some insight into the molecular processes of chain desorption, the number of contacts of the adsorbed chains is monitored with time. For an adsorbed chain (figures 2(*a*) and 3(*a*)) at equilibrium (no flow) after one of its segments diffusionally desorbs from the surface, then either another segment desorbs and the number of contacts reduces, or one of the already free segments adsorbs.

Table 4. The centre of mass diffusion coefficients normal (D_{zz}) and parallel (D_{yy}) to the walls for systems of hexamers under shear. MD units are used throughout, and the width of the film is $h = 6{\cdot}0\sigma$.

$\dot{\gamma}_{\text{wall}}$	D_{zz}			D_{yy}		
	2 cont.[a]	4 cont.	6 cont.	2 cont.	4 cont.	6 cont.
			$\epsilon_w = 1{\cdot}0\epsilon$			
0·009	0·0045	0·0018	0·0013	0·0087	0·0069	0·0063
0·017	0·0047	0·0019	0·0013	0·0092	0·0074	0·0069
0·030	0·0049	0·0020	0·0016	0·0103	0·0081	0·0071
0·048	0·0054	0·0022	0·0018	0·0113	0·0089	0·0095
0·078	0·0071	0·0025	0·0019	0·0148	0·0101	0·0100
0·099	0·0072	0·0028	0·0024	0·0152	0·0125	0·0132
0·144	0·0084	0·0037	0·0026	0·0189	0·0147	0·0155
			$\epsilon_w = 2{\cdot}0\epsilon$			
0·007	0·0019	0·0002	0·0001	0·0036	0·0011	0·0009
0·014	0·0021	0·0003	0·0001	0·0077	0·0011	0·0010
0·021	0·0018	0·0004	0·0001	0·0053	0·0014	0·0013
0·055	0·0024	0·0005	0·0002	0·0066	0·0034	0·0026
0·087	0·0069	0·0007	0·0003	0·0129	0·0041	0·0044

[a] cont. = contact.

These motions are just diffusional motions biased by the attractive wall potential and the chain connectivity, and the result is a struggling motion on top of the wall with a lot of segments desorbing and readsorbing diffusionally until, after some time, all the segments are 'free'. This kind of motion is characterized by large fluctuations of the number of adsorbed segments (contacts) as the energy barrier for desorption is comparable to the kinetic energy of the segments ($k_BT = 1{\cdot}0\epsilon$ and $\epsilon_w = 1{\cdot}0\epsilon$), and results in a very gradual desorption of the chain from the surface (figure 2(*a*)). On average, a fully adsorbed hexamer desorbs from the surface after 120×10^3 time steps. So, during the time of the simulation (i.e., $\sim 10^6$ time steps) most fully adsorbed chains not only manage to desorb, but spend some time as 'free' chains, or move to the opposite wall and adsorb there, or readsorb on the same surface. For example, the chain in figure 2(*a*) desorbs and then fully adsorbs again four times during the simulated time. For a hexamer near a strongly physisorbing surface ($\epsilon_w = 2$) at equilibrium, the picture is qualitatively the same, with segments diffusionally desorbing and readsorbing, but the fluctuations of number of contacts with time are less frequent since now the excess adhesive energy between a solid particle and a chain segment is $\epsilon_w = 2k_BT$ (figure 3(*a*)). Furthermore, only a few (less than 20%) of the fully adsorbed chains manage to desorb in the time scale of the simulation ($0{\cdot}8 \times 10^6$ time steps). A further increase of the wall attraction ($\epsilon_w = 3{\cdot}0\epsilon$) results in the same behaviour but even more slowed down; as a result none of the adsorbed chains with 5 or 6 adsorbed segments desorbs for these times ($\sim 10^6$ time steps), i.e., adsorption on these surfaces is irreversible for these configurations and for the simulated times.

This picture changes qualitatively when shear is introduced, as the existence of a velocity gradient near the surface becomes a driving force for the chains to stretch parallel to the flow. For partly adsorbed chains, depending on whether there is some free space on the surface adjacent to the adsorbed segments or not, the free segments

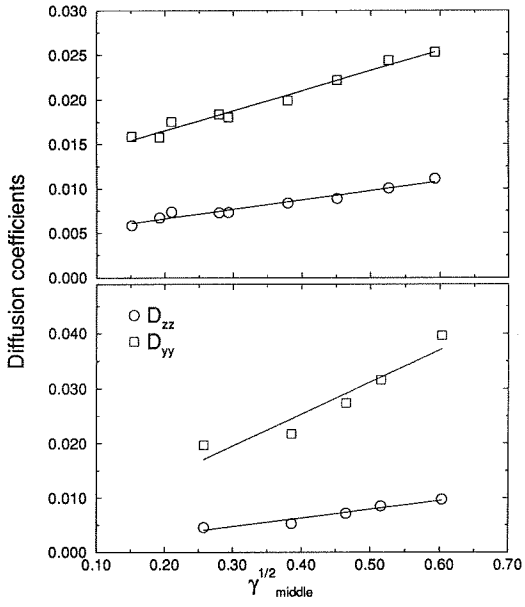

Figure 1. The centre of mass diffusion coefficients of the free chains shown as a function of the square root of the local shear rate in the middle of the pore. The diffusivities normal (circles) and parallel (squares) to the walls are presented for two different wall affinities: top, $\epsilon_w = 1{\cdot}0\epsilon$; bottom, $\epsilon_w = 2{\cdot}0\epsilon$. The lines are least-squares fits.

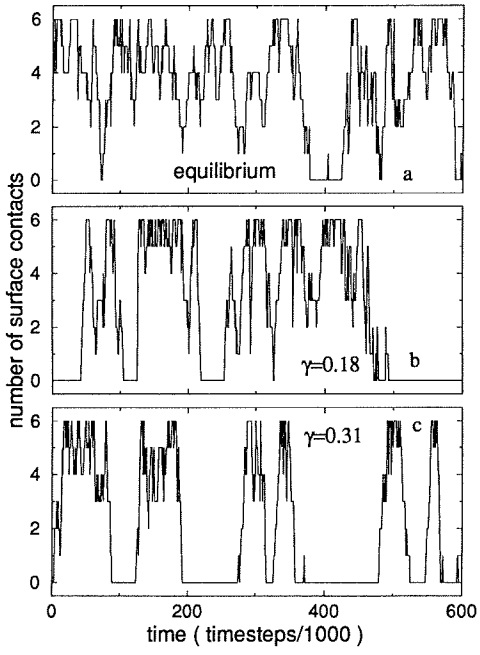

Figure 2. The evolution of number of contacts of a typical fully adsorbed hexamer with the weakly physisorbing surface ($\epsilon_w = 1{\cdot}0\epsilon$) in time for systems (*a*) at equilibrium, (*b*) $\dot{\gamma} = 0{\cdot}18$ and (*c*) $\dot{\gamma} = 0{\cdot}31$.

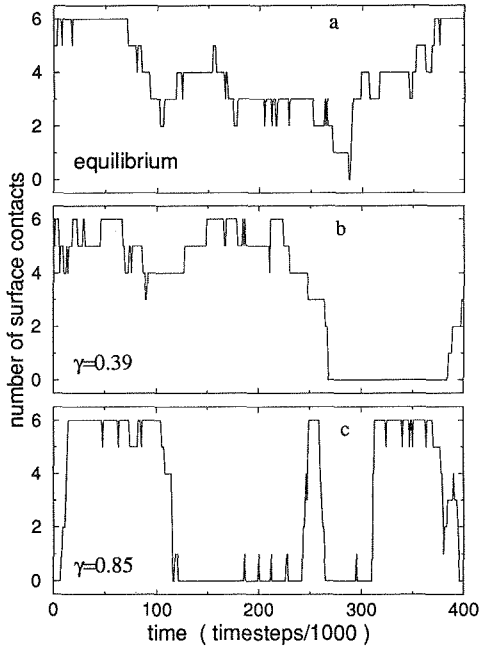

Figure 3. The number of surface contacts of an adsorbed chain (hexamer) on a strongly physisorbing surface versus time ($\epsilon_w = 2{\cdot}0\epsilon$). Three different systems are presented: (*a*) at equilibrium; (*b*) $\dot{\gamma} = 0{\cdot}39$; (*c*) $\dot{\gamma} = 0{\cdot}85$. Although under shear (*b*, *c*) most of the fully adsorbed chains desorb, for the equilibrium system (*a*) one of the few chains that desorbed is presented here (see table 5).

can either adsorb on the surface leading to more contacts with the wall, or the adsorbed segments can be dragged away from the surface to a completely free conformation, since conformations with minimal size parallel to flow are highly favoured by the velocity gradient. But the adsorption and desorption of the chain are taking place simultaneously (in a perpetual exchange process) in such a way that the density near the surface remains dynamically constant, as defined by the wall energy parameter (ϵ_w) and the average fluid density of the film. So the result of shear is to make the actual processes of desorption and adsorption much faster. This can be seen in figures 2(*b*,*c*) and 3(*b*,*c*), where there is a shift from a gradual, slow desorption and adsorption to a much more rapid and highly correlated desorption/adsorption denoted by a systematic change (decrease/increase) in the number of contacts. For the higher shear rates (figures 2(*c*) and 3(*c*)) especially, these processes become very sharp and sudden, denoted by the almost vertical lines going from fully adsorbed to free conformations or the inverse. Moreover, it can be seen in figure 2(*b*,*c*), that the fluctuations in numbers of contacts become much smaller. All these effects result for $\epsilon_w = 1{\cdot}0\epsilon$ in a decrease of the desorption time to 55×10^3 time steps. Near the stronger physisorbing surfaces ($\epsilon_w = 2{\cdot}0$), the same phenomena are observed but to a smaller extent due to the greater adsorption energy barrier. Under shear a considerable fraction of the fully adsorbed chains now desorbs relatively quickly. For example, for a reduced imposed shear rate of $\dot{\gamma} = 0{\cdot}3$, approximately 75% of the fully adsorbed hexamers desorb in 400×10^3 time steps from the $\epsilon_w = 2{\cdot}0$ surface, whereas for the same $\dot{\gamma}$ and $\epsilon_w = 3{\cdot}0$, this fraction is 9%

Table 5. The fraction of fully adsorbed hexamers that desorbed in a certain time period. They are presented as the fraction of desorbed chains to the total number of chains observed in the specific time interval. Averages are over many time origins, so that chains with multiple desorptions are counted properly. The time is measured in thousands of time steps, and the wall velocity (v_w) and shear rate ($\dot{\gamma}$) are given in MD units.

	$\epsilon = 1{\cdot}0\epsilon$				$\epsilon = 2{\cdot}0\epsilon$				$\epsilon = 3{\cdot}0\epsilon$			
v_w	0·0	0·5	0·9	1·5	0·0	0·5	0·9	2·0	0·0	0·5	0·9	2·0
$\dot{\gamma}$	0·0	0·18	0·31	0·54	0·0	0·22	0·39	0·85	0·0	0·22	0·39	0·86
Time												
5	0/157	0/178	2/238	3/199	0/32	0/32	0/41	1/109	0/20	0/25	0/25	0/37
10	1/157	1/177	15/235	19/196	0/32	0/32	0/41	3/109	0/20	0/25	0/25	0/37
20	6/154	18/173	51/234	58/192	0/32	0/32	0/40	6/108	0/20	0/25	0/25	0/36
50	43/150	71/171	127/227	124/183	0/32	0/30	2/39	26/102	0/19	0/25	0/25	0/35
100	82/146	123/165	191/220	163/179	0/31	2/29	4/33	49/97	0/19	0/24	0/25	0/32
200	120/140	150/158	217/219	176/176	3/28	5/25	10/30	77/93	0/18	0/24	0/25	2/30
300	128/137	155/158	219/219	176/176	3/28	8/24	14/27	83/90	0/18	1/24	1/23	3/27
400	134/137	157/157	219/219	176/176	5/28	10/15	18/25	87/89	0/18	1/23	2/23	6/27
500	136/137	157/157	219/219		5/27			88/88	0/18	1/22	2/23	8/27
800	137/137				8/18				0/15	2/20	3/20	16/24

(table 5). This means that, although there now is a mechanism that promotes rapid desorption and adsorption, most of the chains still remain irreversibly adsorbed on the very attractive surface ($\epsilon_w = 3{\cdot}0$).

Furthermore, in all the systems, the chains that desorb abruptly follow a certain *common kinetic pattern*. Taking as an example a fully adsorbed hexamer, one can observe that it remains adsorbed for a long time and occasionally, due to thermal motion one or two segments diffusionally desorb, usually to be pushed towards the surface by a combination of shear and connectivity forces. But there are instances when the diffusional desorption of a segment results in a rapid desorption of the whole chain. Analysing our simulation trajectories it became clear that, in the vast majority of such cases, the end-segment of the coil on the front of the chain (figure 4) is the one which diffusionally desorbs, and then, due to the velocity gradient, moves upwards and towards the back of the chain followed quickly by the adjacent segment; for such a conformation there is an extremely small probability that it will readsorb, as the space on the wall below this tail is occupied by the rest of the coil. Simultaneously, the existence of a tail results in an increased normal size which is unfavourable under flow. Subsequently, the rest of the successive segments can only move away from the surface, resulting in very rapid desorption (figure 4) in a highly correlated manner. For the strongly physisorbing surfaces, the chains that desorb also follow this very abrupt molecular mechanism, although most of the chains are irreversibly adsorbed for the simulated time scales (table 5). Perhaps the most interesting observation concerns the almost complete absence of readsorption of segments belonging to the free part of such a chain during the desorption of the remaining adsorbed segments for sufficiently high shear rates.

For the decamers all of the above is observed as well, but slowed down a little due to the possibility of having even more contacts with the surfaces. Qualitatively the same behaviour as for the hexamers is observed both at equilibrium and under shear (figure 5). Moreover the molecular mechanism of desorption is most of the

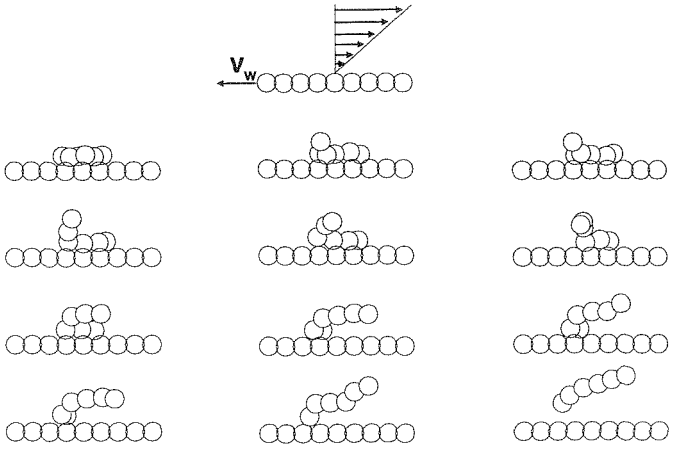

Figure 4. Successive conformations (every 1000 time steps) of a fully adsorbed hexamer desorbing from the $\epsilon_w = 2{\cdot}0$ surface under shear ($\dot{\gamma} = 0{\cdot}39$). A projection on the shear plane is shown, with time increasing from left to right and from top to bottom. The dragging of the front tail by the velocity gradient and the resulting segment-by-segment detachment of the chain result in a molecular mechanism promoting very rapid kinetics in the final stage of desorption.

time the same as for the shorter chains: the front end diffusionally desorbs and the rest of the adsorbed beads follow in a segment-by-segment manner (figure 6). Another characteristic example can be seen in figure 7 where some of the middle segments of the chain have diffusionally desorbed from the wall, thus creating a loop. Owing to the velocity gradient conformations of this kind are unfavourable and are rapidly desorbed. The ultimate desorption is again initiated by the desorption of the front segments. For the rather short chains that we simulate (ten beads per chain), this occurs very infrequently, but it is expected to be fairly typical for longer chains.

Putting together the information from figures 2, 3, and 5 with the chain kinetics from figures 4, 6 and 7 we can build a more complete picture of the dynamics of oligomer desorption and adsorption under shear. The total time it takes for a chain to desorb consists of two parts: first, there are conformational fluctuations of the adsorbed chain on top of the wall until a suitable conformation appears, i.e., a desorbed front tail, and then a very fast, correlated desorption of the complete chain takes place. Naturally, the total desorption time is determined by the slower of the two parts; in the vicinity of strongly adsorbing surfaces and/or under high shear rates the first, 'diffusional', process is slower, whereas for weakly attractive walls and/or low shear rates the second, 'rotational', process is slower. This total desorption time can be defined, for the MD trajectories, as the time between the first instant that a chain becomes adsorbed and the moment that all of its segments are free for the first time. This desorption time is averaged over the simulation on time, over all desorptions observed, and over all chains of the same adsorption energy. In figure 8 we selected those chains with energies of adsorption (number of contacts) that correspond to the average adsorption energy at equilibrium and plotted their desorption times versus the shear rate near the wall ($\dot{\gamma}_{\text{wall}} = (\partial u_x/\partial z)_{\text{wall}}$) taking the slip into account whenever it exists.

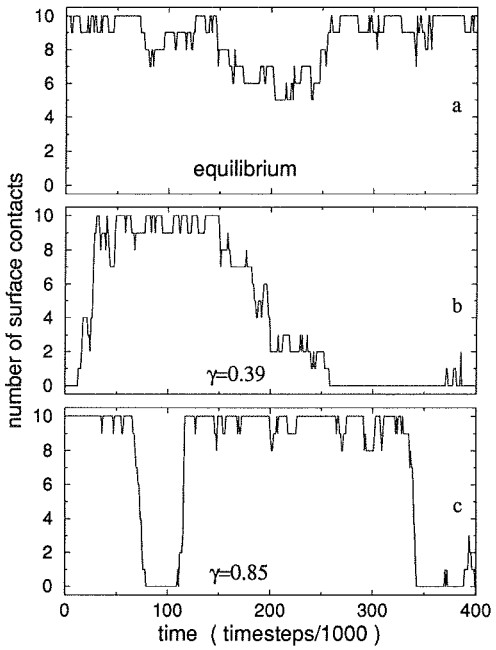

Figure 5. The number of surface contacts of a fully adsorbed decamer versus time for the $\epsilon_w = 2{\cdot}0$ surface. The systems in equilibrium (*a*), and at two different shear rates (*b*) $\dot{\gamma} = 0{\cdot}3$ and (*c*) $\dot{\gamma} = 0{\cdot}5$ are presented. At equilibrium (*a*) although some of the adsorbed segments diffusionally desorb, the chain typically remains adsorbed for the total time of the simulation. Shear (*b*) promotes desorption and, for these shear rates, the time for the diffusional desorption of the front tail is comparable with the time for the final rotational stage of desorption (denoted by a systematic decrease in the number of contacts). For higher shear rates (*c*) the rotational part of desorption, denoted by the almost vertical lines, becomes very rapid, and the desorption time is determined by the slower process of the front tail diffusional detachment.

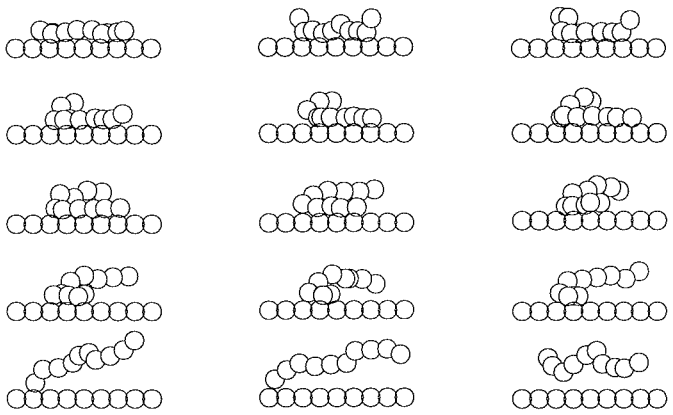

Figure 6. The most predominant molecular mechanism for the kinetics of the final states of desorption of the decamers under shear involves configurations that start with a desorbed front tail and an extremely rapid, correlated, segment-by-segment desorption of the rest of the coil: successive conformations (every 1000 time steps) with time increasing from left to right and from top to bottom ($\epsilon_w = 2{\cdot}0$, $\dot{\gamma} = 0{\cdot}64$).

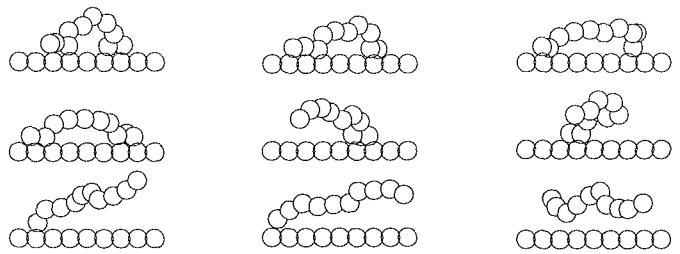

Figure 7. Although the decamer is quite short, a second mechanism of desorption can be observed as well, namely, the 'dragging' of a loop by the velocity gradient. For longer chains (polymers) this is expected to be the most important mechanism by which shear promotes desorption ($\epsilon_w = 2{\cdot}0$, $\dot{\gamma} = 0{\cdot}39$).

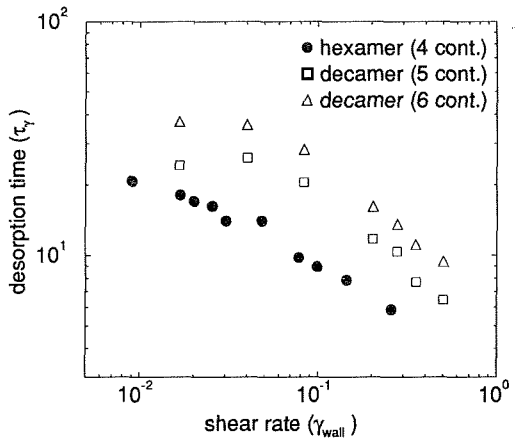

Figure 8. The desorption time versus shear rate for systems with $\epsilon_w = 1{\cdot}0$ surfaces. The desorption times that correspond to the average energy of adsorption (i.e., average number of contacts) are presented (●, hexamers with 4 contacts; and □ and △, decamers with 5 and 6 contacts).

Furthermore, the segment-by-segment, correlated kinetic scheme of desorption shown in figures 4, 6, and 7 resembles strongly conformational scquences of chains under strong rotational diffusion or turbulence. We hestiate though to use the term enhanced rotational diffusion to describe the desorption kinetics, at this point, as there is some very peculiar behaviour near the surfaces; as observed in figures 2, 3, and 5, the rotational diffusion is halted completely for a long time and suddenly, with the appearance of a specific conformation, is dramatically enhanced. On the other hand, this idea can be utilized to model theoretically the desorption kinetics near an attractive surface [30, 31].

4. Conclusion

In this section we summarize our findings concerning the chain mobility near an attractive surface, and the desorption dynamics of oligomer melts confined in spaces comparable with their molecular dimensions, and the influence of shear. The chain mobility, which can be described through the centre of mass diffusion coefficient

tensor, is decreased in the vicinity of an adsorbing surface. This slowdown depends on the wall affinity and ranges *from moderate* next to weakly physisorbing surfaces (a factor of 4 for $\epsilon_w = 1$) *up to three orders in magnitude* near strongly physisorbing surfaces ($\epsilon_w = 3$). These trends are in very good agreement with the decrease in the relaxation times of oligomers next to similar surfaces, which were shown to originate from an increase in density near the wall rather than from the bare adhesive energy barriers of the surface–segment potential [16]. This reduced mobility can explain the dramatic increase in the effective viscosity in nanoscopically confined systems observed experimentally [2–5, 14], expecially if one takes into account that the mica surfaces used in these experiments are characterized by very strong affinities for most of the chemical systems studied [2].

As far as the desorption is concerned, at equilibrium (no flow) we find a diffusional, gradual process in which, due to thermal motion, every segment can desorb from the surface and subsequently can randomly remain free or readsorb. This results in a struggling motion of the chains on the adsorbing surface. Depending on the wall attraction an oligomer can desorb relatively quickly ($\epsilon_w = 1{\cdot}0 k_B T$) or, as the energy of adsorption becomes larger than $k_B T$, the desorption can become limited ($\epsilon_w = 2{\cdot}0$), or extremely slow (for $\epsilon_w = 3{\cdot}0$ the fully adsorbed oligomers are irreversibly adsorbed on the time scale of our simulations).

When shear is introduced to a melt of oligomers there is a tendency for the chains to stretch parallel to the flow; when this melt is confined, the geometrical constraint of the surface enhances this process. For the adsorbed coils this results in a systematic increase in the fraction of chains with many contacts with the surfaces, and thus the average energy of adsorption per chain increases with shear. At the same time, desorption is promoted, both by the shear enhanced diffusivities normal to the walls and by the appearance of a rapid ultimate stage of chain detachment, even though the energy that binds the coils to the surfaces increases. Furtheremore, the ultimate stage of desorption follows a common kinetic pattern which involves a rapid, correlated, segment-by-segment desorption of the oligomer.

It should be noted that although this molecular process of rotational desorption is very rapid, the total desorption time can be determined by the diffusional desorption of the front tail from the surface, when this is slower (figure 5(*c*)). But since diffusion is also enhanced by shear both in the bulk (figure 1) and in the vicinity of an attractive surface (table 4), the desorption time again decreases with shear rate. For example, in the case of weakly attractive surfaces ($\epsilon_w = 1$) for chains with 6 contacts, the decrease in desorption time is determined completely by the shear enhanced mobility (a twofold increase of the D_{zz} results in a twofold decrease of the desorption time), but for the chains with 4 contacts, the shear enhanced self-diffusion of the oligomers alone is insufficient to account for the decrease of the desorption time; D_{zz} increases by a factor of 2 (table 4) whereas the desorption time decreases by a factor of 4 (figure 8). In the case of strongly attractive surfaces ($\epsilon_w = 2$) the, latter situation becomes even more obvious. For example, for chains with 4 contacts, the diffusivity normal to the walls is enhanced by a factor less than 4, in comparison with the equilibrium value (table 4), whereas the desorption time decreases by a factor of 13.

Keeping in mind that there is a continuous exchange of chains in the surface–melt interface, all the changes described here for the desorption are simultaneously mirrored by equivalent changes in the adsorption processes. In the case of oligomers, that we study here, the predominant mechanism is due to forces acting on the tails,

but as the chain length increases, there exists a significant force on loops as well, which we expect to be the main one for long polymer chains.

At this point, it should be mentioned that shear may affect the structure of certain films in much more intricate ways than that suggested here. In particular, under different conditions of pressure, density and wall symmetry, the confinement could lead to 'solidification' near the surfaces, manifested by the existence of domains with crystalline ordering [32]. In these systems shear may affect the structure of these domains resulting in a destruction of their crystallinity, thus causing the melting of these 'microcrystallines'. On the other hand, the results presented in this study are more directly related to effects occurring in films with a disordered (glassy or fluid) structure inside the solid–oligomer interface [16].

Finally, we comment on the correspondence between our very flexible model chains and real polymer molecules. Obviously our model is rather generic, although it has proved to be very effective in capturing the response of polymeric coils in a variety of systems. The lack of any intramolecular architecture, such as bond angles, dihedral potentials etc., results in great flexibility, and the best way to relate our model to real polymers is to compare the Kuhn segment of our model with that of a specific real polymer molecule. This leads to an 'equivalence' of our segment with several real monomers [21]. Overall, we believe that the molecular mechanisms observed for our model describes the response of real chains qualitatively, but the time scales involved will depend strongly on system specific physical and chemical properties.

This research was supported by the Netherlands Foundation of Technology (SON-STW) and the Netherlands Organization for Scientific Research (NWO) through the Russian–Dutch exchange programmes. Support from IBM Netherlands and IBM Research Division is also acknowledged.

References

[1] ISRAELACHVILI, J., 1991, *Intermolecular and Surface Forces, 2nd Edn* (San Diego: Academic Press).
[2] GEE, M. L., MCGUIGGAN, P. M., ISRAELACHVILI, J. N., and HOMOLA, A. M., 1990, *J. chem. Phys.*, **93**, 1895.
[3] HU, H., CARSON, G. A., and GRANICK, S., 1991, *Phys. Rev. Lett.*, **66**, 2758.
[4] KLEIN, J., PERAHIA, D., and WARBURG, S., 1991, *Nature*, **352**, 143.
[5] HOMOLA, A. M., NGUYGEN H. V., and HADZIIOANNOU, G., 1991, *J. chem. Phys.*, **94**, 2346.
[6] TEN BRINKE, G., AUSSERRE, D., and HADZIIOANNOU, G., 1988, *J. chem. Phys.*, **89**, 4374.
[7] BITSANIS, I., and HADZIIOANNOU, G., 1990, *J. chem. Phys.*, **92**, 3827.
[8] THOMPSON, P. A., GREST, G. S., and ROBBINS, M. O., 1992, *Phys. Rev. Lett.*, **68**, 3448.
[9] RIBASKY, M. W., and LANDMAN, U., 1992, *J. chem. Phys.*, **97**, 1937.
[10] HORN, R. G., and ISRAELACHVILI, J. N., 1981, *J. chem. Phys.*, **75**, 1400.
[11] HORN, R. G., HIRZ, S. J., HADZIIOANNOU, G., FRANK, C. W., and CATALA, J. M., 1989, *J. chem. Phys.*, **90**, 6767.
[12] SCHOEN, M., DIESTLIER, D. J., and CUSHMAN, J. H., 1987, *J. chem. Phys.*, **87**, 5464.
[13] HANSEN, J., and MCDONALD, I., 1986, *Theory of Simple Liquids* (London: Academic Press).
[14] GRANICK, S., 1991, *Science*, **253**, 1374.
[15] VAN ALSTEN, J., and GRANICK, S., 1990, *Macromolecules*, **22**, 3143.
[16] BITSANIS, I., and PAN, C., 1993, *J. chem. Phys.*, **99**, 5520.
[17] THOMPSON, P. A., and ROBBINS, M. O., 1990, *Science*, **250**, 792.
[18] LUPKOWSKI, M., and VAN SWOL, F., 1991, *J. chem. Phys.*, **95**, 1995.

[19] MANIAS E., HADZIIOANNOU G., and TEN BRINKE, G., 1994, *J. chem. Phys.*, **101,** 1721.
[20] GREST, G. S., and KREMER, K., 1986, *Phys. Rev. A*, **33,** 3628.
[21] KREMER, K., and GREST, G. S., 1990, *J. chem. Phys.*, **92,** 5057.
[22] MANIAS, E., HADZIIOANNOU, G., BITSANIS, I., and TEN BRINKE, G., 1993, *Europhys. Lett.*, **24,** 99.
[23] BERENDSEN, H. J. C., POSTMA, J. P. M., VAN GUNSTEREN, W. F., DINOLA, A., and HAAK, J. R., 1984, *J. chem. Phys.*, **81,** 3684.
[24] PELLETIER, E., BELDER, G. F., STAMOULI, A., TEN BRINKE, G., and HADZIIOANNOU, G., 1995, *Science* (submitted).
[25] DAIVIS, P., and EVANS, D. J., 1994, *J. chem. Phys.*, **100,** 541.
[26] WINKLER, R. G., MATSUDA, T., and YOON, D. Y., 1993, *J. chem. Phys.*, **98,** 729.
[27] ALLEN, M. P., and TILDESLEY, D. J., 1990, *Computer Simulation of Liquids* (Oxford: Clarendon Press).
[28] CIEPLAK, M., SMITH, E. D., and ROBBINS, M. O., 1994, *Science*, **265,** 1209.
[29] CUMMINGS, P. T., WANG, B. Y., FRASER, K. J., and EVANS, D. J., 1991, *J. chem. Phys.*, **94,** 2149.
[30] SUBBOTIN, A., SEMENOV, A., MANIAS, E., TEN BRINKE, G., and HADZIIOANNOU, G., 1995, *Macromolecules*, **28**, 3898.
[31] SUBBOTIN, A., SEMENOV, A., MANIAS, E., HADZIIOANNOU, G., and TEN BRINKE, G., 1995, *Macromolecules*, **28,** 1511.
[32] KOOPMAN, D. C., GUPTA, S., BALLAMUDI, R. K., WESTERMAN-CLARK, G. B., and BITSANIS, I. A., 1994, *Chem. Engng Sci.*, **49,** 2907.